

UCRL-JC-124044

PREPRINT

CONF-960163--36

**Comparison of soft and hard tissue ablation with sub-ps and ns pulse lasers**

L. B. Da Silva, B. C. Stuart, P. M. Celliers, T. D. Chang, M. D. Feit,  
M. E. Glinsky, N. J. Heredia, S. Herman, S. M. Lane, R. A. London  
D. L. Matthews, J. Neev, M. D. Perry, A. M. Rubenchik

RECEIVED

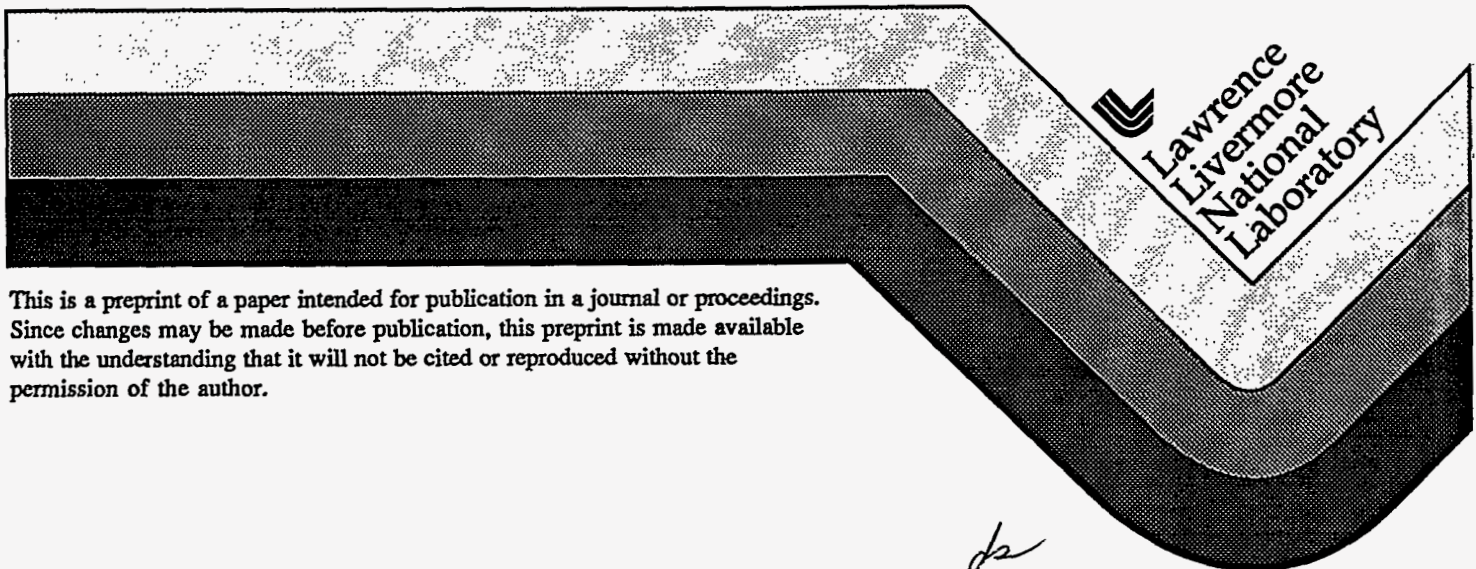
JUN 27 1996

OSTI

This paper was prepared for submittal to the  
Society of Photo-Optical Instrumentation Engineers '96 Conference  
San Jose, CA  
January 28-February 2, 1996

MASTER

May 1996



This is a preprint of a paper intended for publication in a journal or proceedings. Since changes may be made before publication, this preprint is made available with the understanding that it will not be cited or reproduced without the permission of the author.

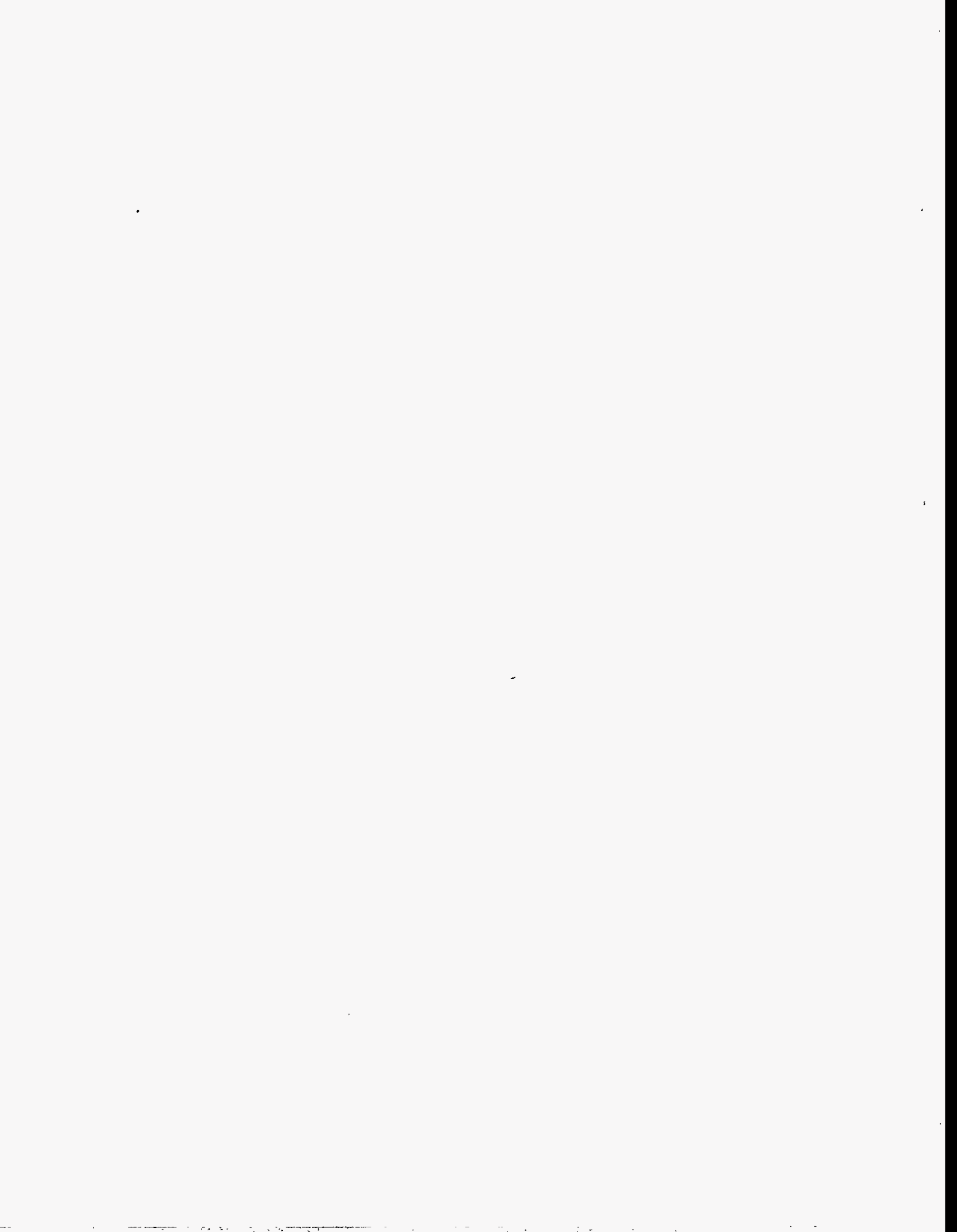
*ds*  
DISTRIBUTION OF THIS DOCUMENT IS UNLIMITED

**DISCLAIMER**

**Portions of this document may be illegible  
in electronic image products. Images are  
produced from the best available original  
document.**

### **DISCLAIMER**

This report was prepared as an account of work sponsored by an agency of the United States Government. Neither the United States Government nor any agency thereof, nor any of their employees, makes any warranty, express or implied, or assumes any legal liability or responsibility for the accuracy, completeness, or usefulness of any information, apparatus, product, or process disclosed, or represents that its use would not infringe privately owned rights. Reference herein to any specific commercial product, process, or service by trade name, trademark, manufacturer, or otherwise does not necessarily constitute or imply its endorsement, recommendation, or favoring by the United States Government or any agency thereof. The views and opinions of authors expressed herein do not necessarily state or reflect those of the United States Government or any agency thereof.



## Comparison of soft and hard tissue ablation with sub-ps and ns pulse lasers

L.B. Da Silva, B.C. Stuart, P.M. Celliers, T.D. Chang\*, M.D. Feit, M.E. Glinsky, N.J. Heredia, S. Herman, S.M. Lane, R.A. London, D.L. Matthews, J. Neev<sup>†</sup>, M.D. Perry and A.M. Rubenchik

Lawrence Livermore National Laboratory, M/S L-399, P.O. Box 808, Livermore CA 94550

\*Department of Veterans Affairs, Northern California Health Systems, 150 Muir Road, Martinez, CA 94553

<sup>†</sup>Beckman Laser Institute and Medical Clinic, 1002 Health Sciences Road East, Irvine, CA 92715  
phone: (510) 423-9867, FAX: (510) 424-2778, email: dasilvaluiz@llnl.gov

### ABSTRACT

Tissue ablation with ultrashort laser pulses offers several unique advantages. The nonlinear energy deposition is insensitive to tissue type allowing this tool to be used for soft and hard tissue ablation. The localized energy deposition leads to precise ablation depth and minimal collateral damage. In this paper we will report on our efforts to study and demonstrate tissue ablation using an ultrashort pulse laser. The ablation efficiency, and extent of collateral damage for 0.3 ps and 1000 ps duration laser pulses will be compared. Temperature measurements of the rear surface of a tooth section will also be presented.

**Keywords:** laser ablation, ultrashort pulse, dentistry, plasma ablation, collateral damage

### 1. INTRODUCTION

Plasma mediated ablation remains one of the few techniques for cutting and processing transparent tissue. It has over the years been studied extensively for a wide variety of laser conditions<sup>1-5</sup>. In this process the laser energy is absorbed by electrons which through collisions transfer energy to other electrons, thereby further ionizing the material, and also transfer energy to ions, thereby leading to melting and vaporization. For nanosecond pulse duration, optical breakdown can be initiated by heating and subsequent free electron generation of absorbing impurities. At the femtosecond pulse duration range this mechanism can also occur but in addition the probability of multiphoton ionization is significantly increased due to the higher peak intensities<sup>6</sup>. In Figure 1. we show a schematic of the process and the important interaction regions. Laser light is absorbed in the produced plasma which can expand out at velocities of approximately  $10^7$  cm/s. The shock waves generated by the high pressure pulse travel at velocities near  $10^6$  cm/s. In a nanosecond the plasma can expand  $\sim 100$   $\mu\text{m}$  and lead to a decoupling between the ablation front and the critical density surface where most of the laser energy is absorbed. In addition, this expanded plasma plume can absorb energy which increases it's expansion velocity but contributes very little to surface ablation. The shock wave propagates approximately 10  $\mu\text{m}$  during the laser pulse and will propagate significantly further before the rarefaction wave traveling from the front surface can reduce the pressure pulse. By contrast for 1 picosecond pulse the plasma can expand 0.1  $\mu\text{m}$  and the shock wave 0.01  $\mu\text{m}$ . Effectively the tissue and plasma are stationary during a sub ps laser pulse. This ensures energy couples into the high density material and minimizes the extent of the high pressure pulse. Thermal timescales are long and consequently heating of the material will be sensitive to the total deposited energy per pulse. High ablation efficiencies reduce the required per pulse energy and as we will show reduce the temperature increase for short pulse irradiation. We will show qualitatively how the ablation craters differ for short and long pulse irradiation and how sub-ps lasers can play an important role in dental ablation.

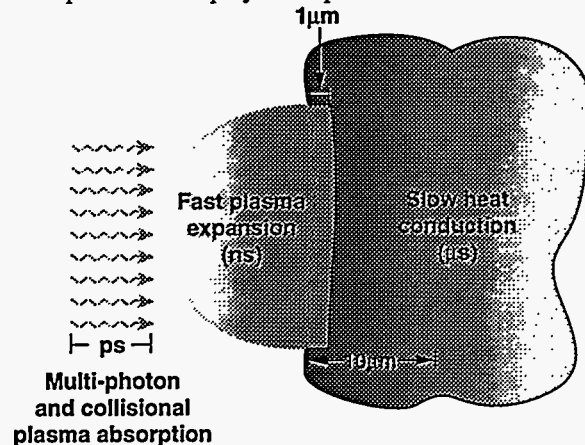


Fig. 1. Relevant Timescales and scalelengths in plasma mediated ablation.

## 2. LASER SYSTEM WITH TUNABLE PULSE LENGTH

In the experiment a 1053-nm Ti:sapphire CPA system<sup>7</sup> diagrammed in Fig. 2 was used as the laser source. Seed pulses of 100 fs from a Kerr-lens mode-locked, Ti:sapphire oscillator were stretched to 1 ns in a four-pass, single-grating (1740 line/mm) pulse stretcher. After amplification to 60 mJ the pulses are compressed in a four-pass, single-grating (1740 line/mm) compressor of variable length. By varying the dispersive path length of the compressor, we obtained pulses of continuously adjustable duration from 0.3 ps to 1000 ps (all reported pulsewidths are intensity full-width at half-maximum). The temporal profile of the compressed pulses depends strongly on the spectral and temporal profile of the stretched pulse. For these measurements, we compressed a near-Gaussian spectral profile to obtain temporally smooth top-hat output pulses. This allowed us to relate the time evolution of the pulse intensity to the measured fluence. This system operated at 10 Hz but single pulse irradiation was also possible.

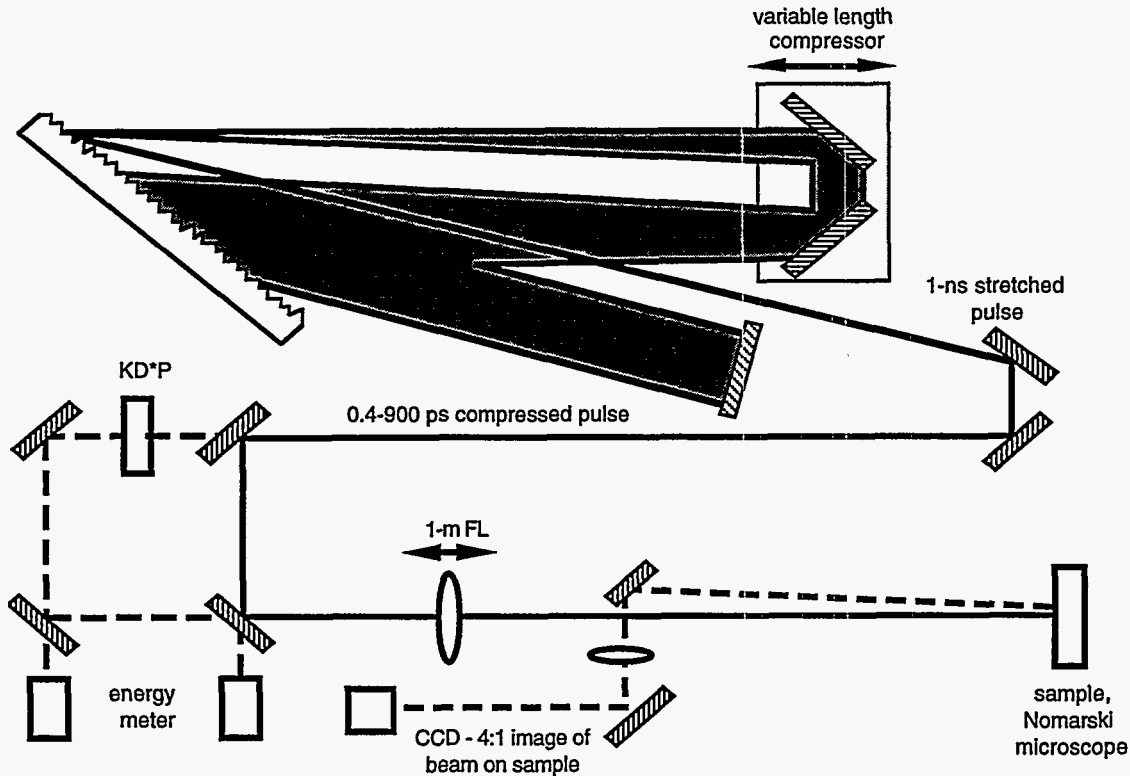


Fig. 2. Experimental set up: Laser, tissue holder, transducer, microscope, scope, computer.

The energy of each pulse was monitored with the leakage through a 92% reflectivity mirror. The rms energy stability was typically less than 3%, and we report the average value here. Due to saturated amplification in the regenerative amplifiers, the maximum energy never exceeded the average by more than 6%. The laser beam was focused onto the sample using a 1-meter focal length lens. The laser spot was monitored with a CCD camera and the spatial mode at the sample had a 98% or better fit to a Gaussian of 0.5 mm FWHM. Our estimated absolute uncertainty in fluence was 15%, but relative values should be within 5%.

## 3. EXPERIMENTAL RESULTS

### 3.1. Ablation measurements

In order to measure the damage fluence and ablation efficiencies samples were mounted and irradiated at a range of fluences and laser pulse durations. After irradiation, a Nomarski microscopy was used to inspect the sample for crater formation. We defined the ablation threshold as the fluence at which a visible crater was produced after 10 pulses. Many fluence levels (5-10) were examined above and below the ablation threshold for a given pulsewidth in order to establish the threshold value. In Fig. 3, we present the results of damage measurements for gels with different linear absorption previously

reported in the paper by Oraevsky et al.<sup>6</sup>. The 7% collagen gels were made of gelatin AG2500 (Sigma, St. Louis, MO) sonicated in a hot water at 60°C and then cooled down to room temperature. Aqueous solutions of Cupric Chloride with low medium and high concentrations were used to produce phantom tissues with low ( $\mu_a=0.01 \text{ cm}^{-1}$ ), medium ( $\mu_a=22 \text{ cm}^{-1}$ ) and high ( $\mu_a=1000 \text{ cm}^{-1}$ ) absorptivity at 1064 nm. Thin slabs of gels with dimensions of 25 mm x 25 mm x 1 mm were prepared for experiments. Figure 3 illustrates one of the key aspects of short pulse irradiation. Specifically, the damage thresholds for transparent and opaque materials converge at shorter pulselengths. Thus, tissue removal will be less sensitive to the type of tissue, coating of the sample, and contamination of the sample for ultrashort pulses. This has important ramification for surgical procedures where strong absorption differences exist and high irradiation fluences could lead to collateral damage.

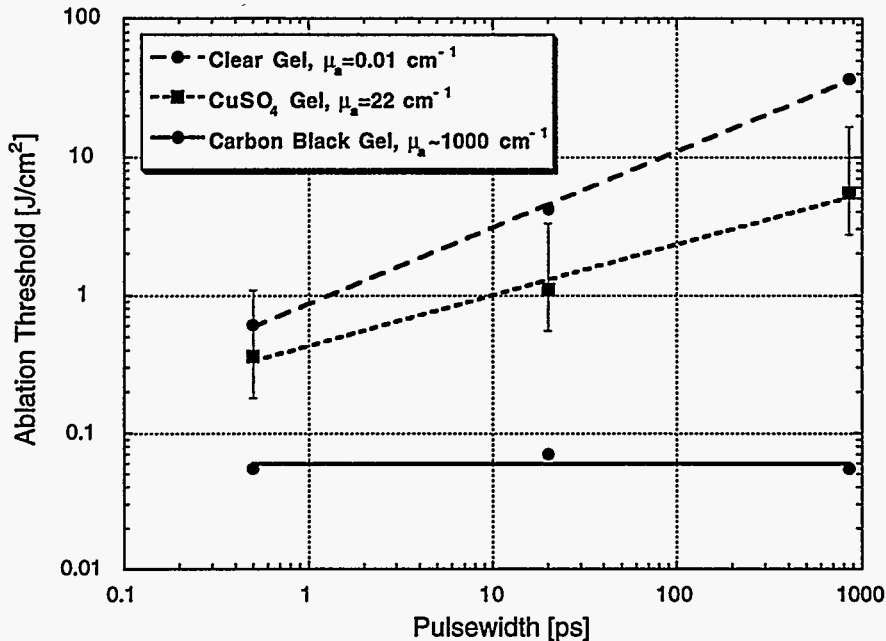


Fig. 3. Ablation threshold fluence as a function of laser pulse duration for various materials: (a) collagen gel ( $\mu_a=0.01 \text{ cm}^{-1}$ ), (b) collagen gel ( $\mu_a=22 \text{ cm}^{-1}$ ), (c) collagen gel ( $\mu_a=1000 \text{ cm}^{-1}$ ).

In order to evaluate the relative efficiencies of short and long pulse irradiation we measured the fluence required to ablate 1  $\mu\text{m}$ /pulse of gel and enamel. In this experiment the ablation rate was measured by doing 100 to 500 shots on the sample and then measuring the crater depth using the Nomarski microscope. The depth of the crater could be measured to  $\pm 2 \mu\text{m}$ . In Fig. 4 we show the required fluence for the two materials and pulse durations. For both materials the short pulse efficiency is an order of magnitude higher. As we previously discussed the primary reason for this is that in long pulse ablation more of the energy goes into heating and expanding the low density plasma than vaporization of the high density material.

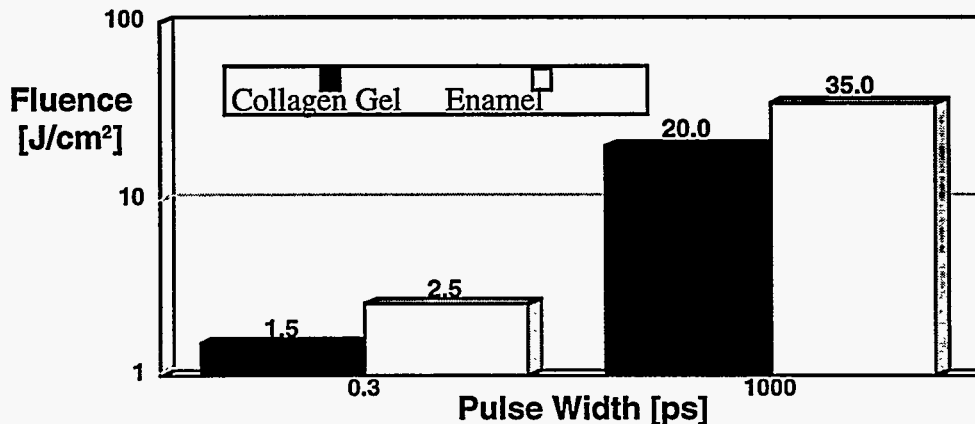


Fig. 4. Necessary fluence to achieve 1 $\mu\text{m}$ /pulse ablation rates of clear collagen gel ( $\mu_a=0.01 \text{ cm}^{-1}$ ), and enamel.

The craters produced by laser ablation show clear differences between short pulse and long pulse irradiation. In Figures 5 we show typical craters produced in collagen gels. For short pulse irradiation a clean smooth crater is produced with no evidence of thermal or mechanical collateral damage. In Figure 6 we compare the ablation craters produced in tooth enamel. Again short pulse ablation produces clean craters with no evidence of cracking and no thermal damage away from the crater site. In contrast, long pulse irradiation shows irregular craters and large cracks produced by thermal and mechanical stresses generated during the ablation process. Similar results were obtained when other tissue types including bone, cartilage, nail and heart tissue were ablated.



Fig. 5. Craters produced in clear collagen gel by 0.3 ps (left) and 1000 ps (right) laser pulses.

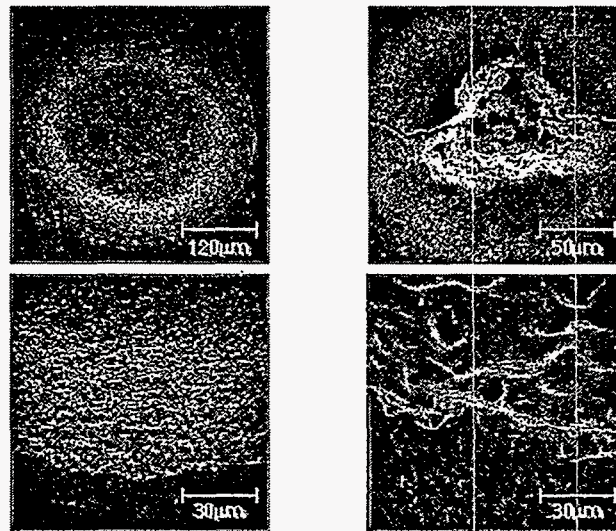


Fig. 6. Craters (and edge of craters) produced in enamel by 0.3 ps (left) and 1000 ps (right) laser pulses.

In addition, to producing clean craters the sharp threshold and accurate ablation rate allows us to easily model the shape of the ablation crater produced by short pulse ablation. From experimental measurements we find that ablation rate can be approximated by the expression

$$a = \begin{cases} a_o \frac{I - I_{Th}}{I} & \text{for } I > I_{Th} \\ 0 & \text{for } I < I_{Th} \end{cases} \quad (1)$$

where  $I$  is the surface intensity and  $I_{Th}$  is the threshold intensity. For dentin  $I_{Th} \sim 1.5 \times 10^{12}$  W/cm<sup>2</sup> and  $a_o \sim 1.5$  µm. It's important to note that the surface intensity changes as the crater is drilled and can be related to the laser beam profile  $I_0$  by the expression  $I = I_0 \cos(\theta)$  where

$$\cos \theta = \frac{1}{\sqrt{\left(\frac{\partial z}{\partial r}\right)^2 + 1}}$$

and  $z(r)$  is the crater shape. In Figure 7 we show the crater evolution using this model and an initial Gaussian beam profile. The calculated shape is in good agreement with the experimentally produced crater also shown in Fig. 7. By



adjusting the initial beam profile it should be possible to tailor the crater shape. Again this is only possible because of the lack of collateral damage in short pulse ablation and the precise ablation rate.

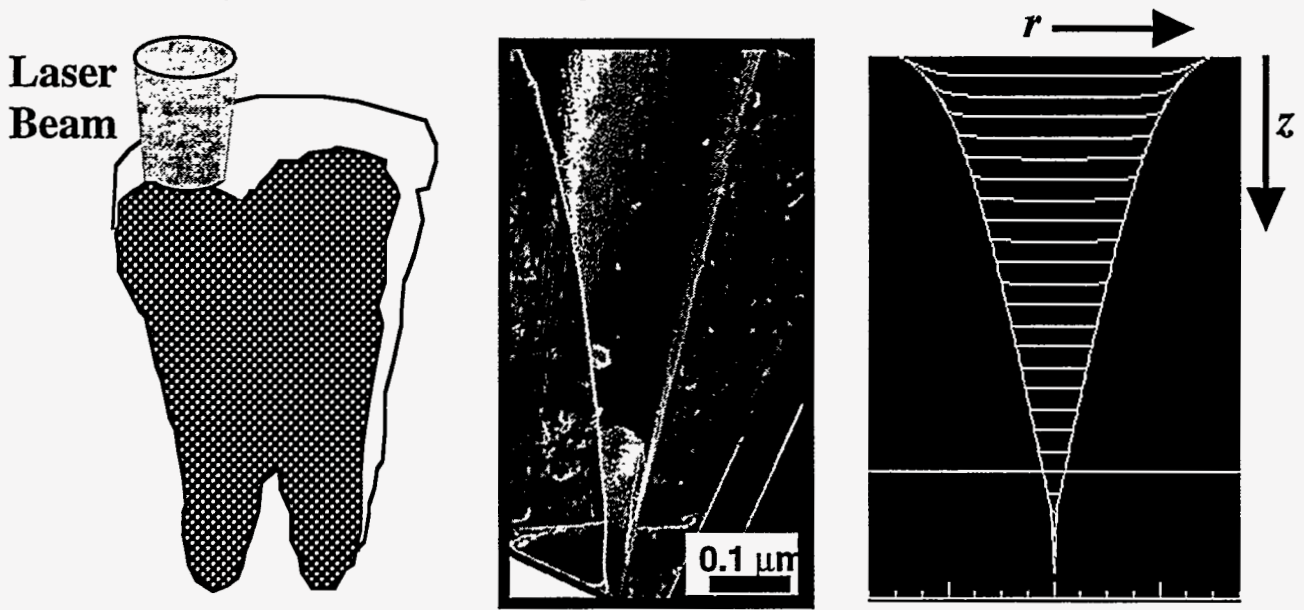


Fig. 7. Irradiation geometry (left) used to study crater shape. Middle picture shows measured crater which has a shape in good agreement with model predictions (right).

### 3.2. Temperature measurements in tooth enamel ablation

In order to measure the deposited energy and assess the possibility of using short pulse laser for dental procedures we performed an experiment to measure the time evolution of the temperature at the rear surface of a 1 mm tooth section during ablation. The temperature was measured using a calibrated infrared camera which directly imaged the rear surface. In Fig. 8 we show the temperature increase at the rear surface of a 1 mm thick section of teeth. During short pulse ablation the temperature increase is 2.5°C. The curve is in good agreement with a three dimensional heat conduction model that assumes a continuous energy deposition of  $\sim 2 \text{ W/cm}^2$  (i.e. 7% of incident energy is left as thermal energy). For long pulse ablation the temperature increase is 20 °C which would limit it's use for dental applications where temperatures increases of 5°C can lead to damage to the pulp. For a more detailed discussion of our modeling of thermal transport in dental ablation see the paper by R.A. London et al. in these proceedings.

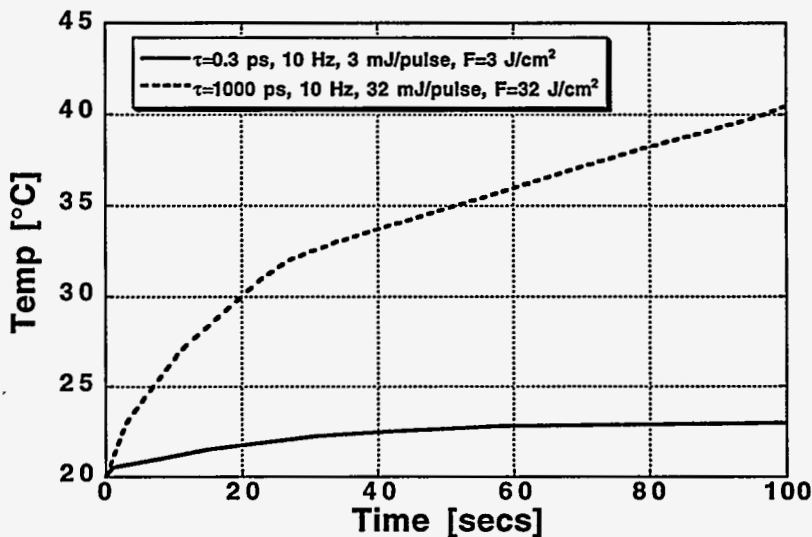


Fig. 8. Temperature evolution at rear surface of 1 mm thick dentin slice for 0.3 ps (solid) and 1000 ps (dashed) laser irradiation.

## 5. CONCLUSION

We have demonstrated experimentally the advantages of short pulses for soft and hard tissue ablation. First, the ablation threshold is insensitive to the material absorption coefficient. Second, the ablation surface is clean and collateral damage is minimal. Third, the comparatively high ablation efficiency leads to minimum heating of the tissue which could be particularly important for dental applications of this technique.

## 6. ACKNOWLEDGMENTS

This work was performed under the auspices of the US Department of Energy by the Lawrence Livermore National Laboratory under contract W-7405-ENG-48.

## 7. REFERENCES

1. A. Vogel, S. Busch, M. Asiyovogel, *Time-resolved measurements of shock-wave emission and cavitation-bubble generation in intraocular laser surgery with ps- and ns-pulses and related tissue effects*, Proc. SPIE 2391, (1995).
2. R. Birngruber, C.A. Puliafito, A. Gawande, W.-Z. Lin, R.T. Schoenlein, and J.G. Fujimoto, IEEE J. Quantum Electron. QE-23, 1836(1987).
3. B. Zysset, J.G. Fujimoto, C.A. Puliafito, R. Birngruber, and T.F. Deutsch, Lasers in Surgery and Medicine 9, 193 (1989).
4. A.A. Oraevsky, R.O. Esenaliev, S.L. Jacques, and F.K. Tittel, *Mechanism of precise tissue ablation with minimal side effects (under confined-stress conditions of irradiation)*, Proc. SPIE 2323, 250(1994).
5. A.A. Oraevsky, V.S. Letokhov, and R.O. Esenaliev: Pulsed laser ablation of biological tissues. Review of ablation mechanisms. IN: Lecture Notes in Physics, ed. by JC Miller, Springer Verlag, Berlin-New York-London-Paris-Tokyo, 1991 (Proceeding of the Workshop "Laser Ablation: Mechanisms and Applications, April 1991, Oak Ridge, TN).
6. A.A. Oraevsky, L.B. Da Silva, M.D. Feit, M.E. Glinsky, B.M. Mammini, K.L. Paquette, M.D. Perry, A.M. Rubenchik, B.C. Stuart, *Plasma mediated ablation of biological tissues with ultrashort laser pulses*, Proc. SPIE 2391, 423(1995).
7. B.C. Stuart, S. Herman, and M.D. Perry, IEEE J. Quantum Electron. 31, 528(1995).